

Concepts for Experiments at Future Colliders I

PD Dr. Oliver Kortner

18.11.2024

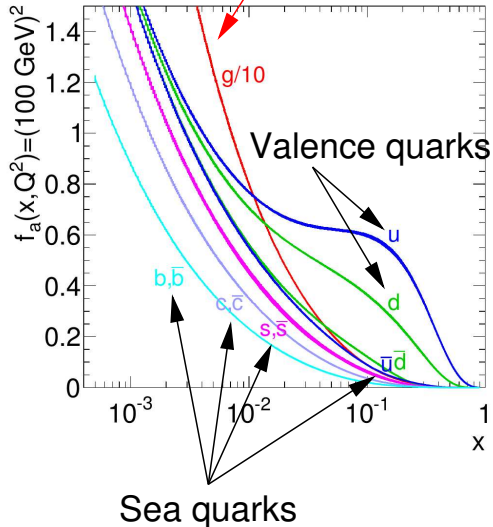
Recapitulation of the previous lecture

Parton densities

Let us move to hadron (pp) colliders!

Gluons

MSTW08



- x : Fraction of the proton momentum carried by a single parton.
- Q : Momentum scale of the parton collision.

$$\sqrt{s_{Parton\ 1, Parton\ 2}} = \sqrt{x_1 \cdot x_2} \sqrt{s_{pp}},$$

i.e. collisions with

$$\sqrt{s_{Parton\ 1, Parton\ 2}} = \sqrt{s_{pp}} \text{ are very rare.}$$

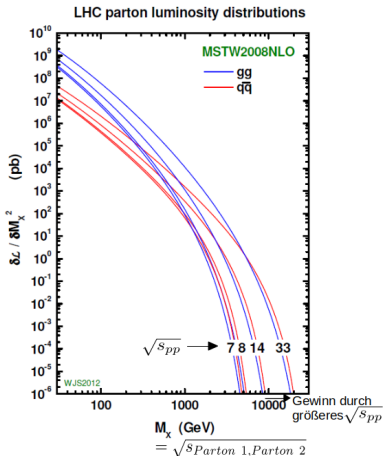
Recapitulation of the previous lecture

Parton luminosity

General formula for the cross section of a process:

$$\sigma_{pp \rightarrow X} = \sum_{a,b=q,g} \int_0^1 \int_0^1 \hat{\sigma}_{ab \rightarrow X} \cdot \underbrace{f_a(x_a, Q^2) \cdot f_b(x_b, Q^2)}_{\text{parton luminosity}} dx_a dx_b$$

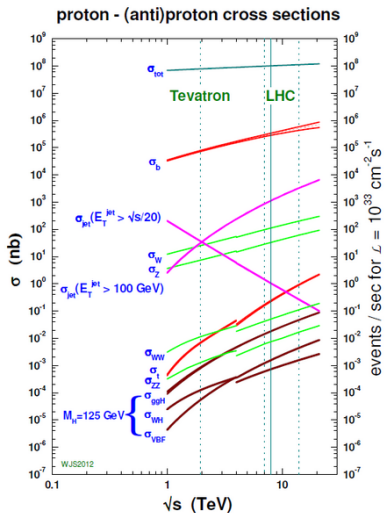
$\hat{\sigma}_{ab \rightarrow X}$: Cross section of the process at parton level.



- Parton luminosities increase with $\sqrt{s_{pp}}$ because more and more sea quarks and gluons will be created.
- Gluons dominate at small values of $\sqrt{s_{parton 1, parton 2}}$ because the parton densities are dominated by gluons at small values of x .

Recapitulation of the previous lecture

Cross sections for pp collisions



- σ increases with $\sqrt{s_{pp}}$.
 - σ for interesting processes like the production of Higgs bosons very small and much smaller than for QCD processes as $pp \rightarrow b\bar{b}$.
- ⇒
- Large pp collision rates (large luminosity) required to become sensitive to rare processes.
 - Selective triggers for the selection of interesting pp collisions mandatory.

Hadron collider strategy for the next years

- Increase the LHC luminosity by an order of magnitude → HL-LHC.
- Increase the centre-of-mass energy $\sqrt{s_{pp}}$ by an order of magnitude → FCC-hh.

Recapitulation of the previous lecture

Future hadron colliders

- HL-LHC: $\sqrt{s} = 14 \text{ TeV}$, $\int \mathcal{L} dt = 3 \text{ ab}^{-1}$
Increase of the LHC's luminosity by an order of magnitude with improved beam optics in the collision zones.
- FCC-hh: $\sqrt{s} = 100 \text{ TeV}$, $\int \mathcal{L} dt = 30 \text{ ab}^{-1}$
Increase of the center-of-mass energy with a new storage ring of the four times the circumference of the LHC ring and dipole magnets with twice the field strength.

Most important goals of the physics programmes (without details)

- HL-LHC
 - Measurement of the properties of the Higgs boson, in particular observation of the decay $H \rightarrow \mu^+ \mu^-$ and of first evidence of Higgs boson pair production.
 - Search for physics beyond the Standard Model.
- FCC-hh
 - Precision measurements of Higgs boson properties, especially the study of the Higgs boson pair production for the exploration of the structure of the Higgs boson self-coupling.
 - Search for physics beyond the Standard Model.

Recapitulation of the previous lecture

Conceptual design of the FCC ring

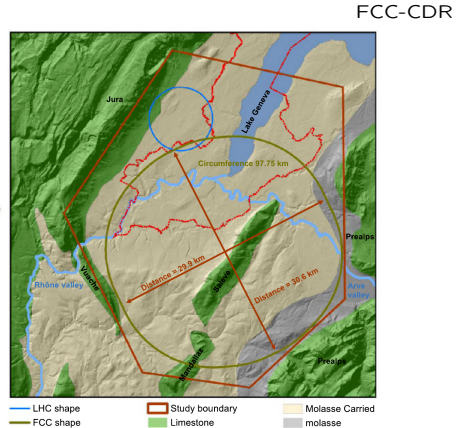
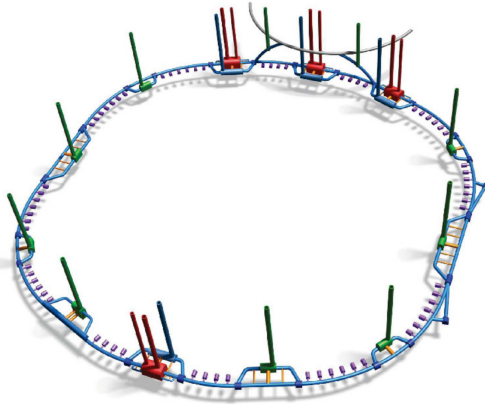


Fig. 2. Left: 3D, not-to-scale schematic of the underground structures. Right: study boundary (red polygon), showing the main topographical and geological structures, LHC (blue line) and FCC tunnel trace (olive green line).

Recapitulation of the previous lecture

Dipole magnets for the FCC-hh

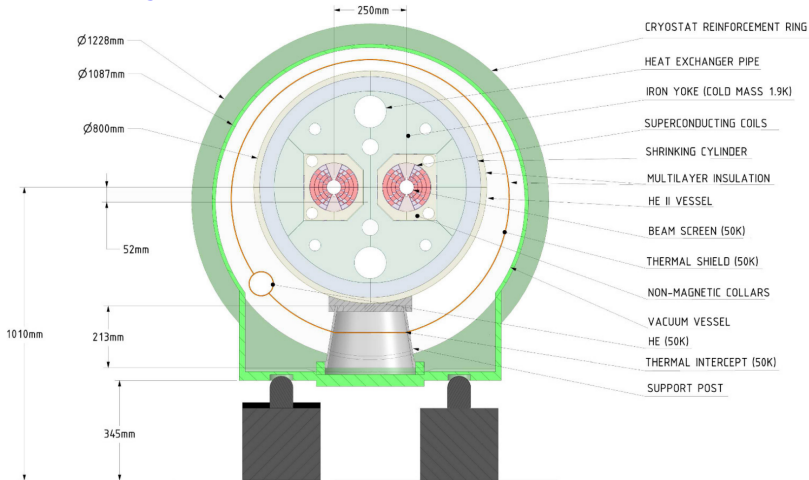


Fig. 3.1. Main dipole cross-section.

- Plan to use Nb_3Sn wires as superconductors in magnets.
- ⇒ Achievable field strength: $16\text{ T} \Rightarrow \sqrt{s} = 100\text{ TeV}$.

Recapitulation of the previous lecture

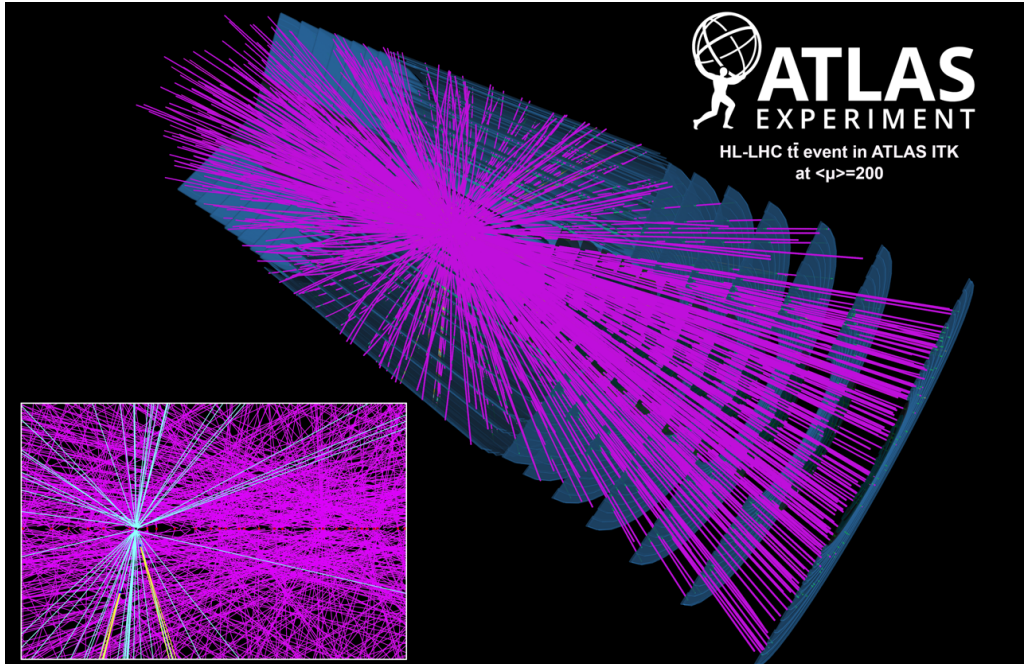
Comparison of the HL-LHC and the FCC-hh

	LHC	HL-LHC	FCC-hh	
			Initial	Nominal
Physics performance and beam parameters				
Peak luminosity ¹ ($10^{34} \text{ cm}^{-2} \text{ s}^{-1}$)	1.0	5.0	5.0	<30.0
Optimum average integrated luminosity/day (fb^{-1})	0.47	2.8	2.2	8
Peak number of inelastic events/crossing	27	135 levelled	171	1026
Total/inelastic cross section σ proton (mbarn)		111/85		153/108
Beam parameters				
Number of bunches n		2808		10 400
Bunch spacing (ns)	25	25		25
Bunch population N (10^{11})	1.15	2.2		1.0

- Similar operating conditions at the FCC-hh in the initial phase like at the HL-LHC.
- ⇒ Detectors which will were developed for the HL-LHC are suitable for the operation at the FCC-hh in phase 1.
- Evolution of the HL-LHC detectors for the areas of very high particle fluxes needed.

Recapitulation of the previous lecture

Example of a collision event at the HL-LHC



Recapitulation of the previous lecture

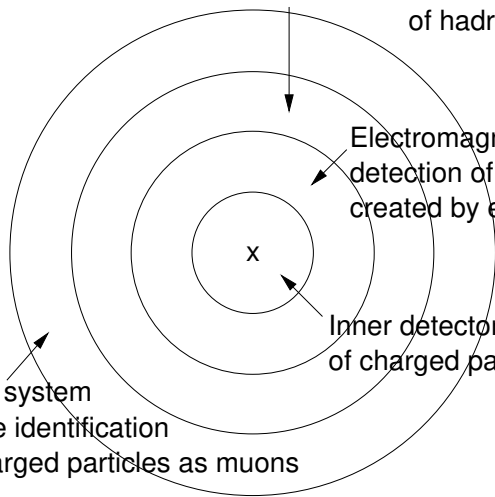
Basic structure of a particle detector at a hadron collider

Hadron calorimeter for the detection
of hadronic showers

Electromagnetic calorimeter for the
detection of electromagnetic showers
created by electrons, positrons, and photons

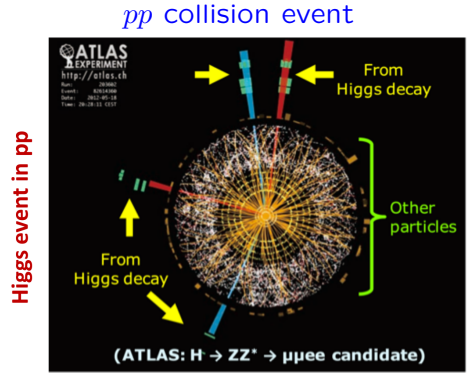
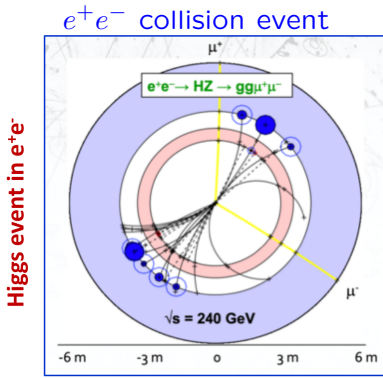
Inner detector for the measurement
of charged particle tracks

Myon system
for the identification
of charged particles as muons



Different operation conditions at e^+e^- and pp colliders

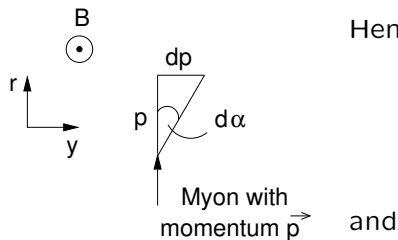
- As explained in the previous lecture, cross sections are much smaller in e^+e^- collision than in pp collisions because only electroweak processes are accessible in the e^+e^- vertex while there is a huge total pp because the partons also interact strongly.
- ⇒ Much smaller particle fluxes and particle multiplicities in the detectors at an e^+e^- than at a pp collider.
- ⇒ Different requirements for the detectors.



Recapitulation of the previous lecture

Charged particle trajectories in the inner detector

$$d\alpha = \frac{dp}{p} = \frac{qvBdt}{p} = \frac{q}{p} B \underbrace{vdt}_{=ds=dr} = \frac{q}{p} B ds.$$



Hence we get

$$\alpha(r) \approx \frac{q}{p} \int_{r_0}^r B(s) ds$$

$$y(r) = \int_{r_0}^r \alpha(r') dr' = \frac{q}{p} \int_{r_0}^r \int_{r_0}^{r'} B(s) ds dr'.$$

Beispiel. $p = 1 \text{ GeV}$. $r_0 = 0$. $B = 2 \text{ T}$.

$\alpha(10 \text{ cm}) = 60 \text{ mrad}$. $y(10 \text{ cm}) = 3 \text{ mm}$.

$\alpha(1 \text{ m}) = 0,6 \text{ rad}$. $y(1 \text{ m}) = 30 \text{ cm}$.

Momentum resolution in the inner detector

- Deflection angle at distance r from the pp interaction point:

$$\alpha(r) = \frac{q}{p} \int_0^r B ds$$

- Total deflection angle: $\alpha := \alpha(r_{max})$ (r_{max} radius of the inner detector).
- Error propagation:

$$\delta\alpha = \frac{|q|}{p^2} \int_0^{r_{max}} B ds \cdot \delta p = \alpha \cdot \frac{\delta p}{p} \Leftrightarrow \frac{\delta p}{p} = \frac{\delta\alpha}{\alpha}$$
$$\frac{\delta p}{p} = \frac{\delta\alpha}{\frac{|q|}{p} \int_0^{r_{max}} B ds}$$

Recapitulation of the previous lecture

Momentum resolution in the inner detector

$$\frac{\delta p}{p} = \frac{\delta \alpha}{\frac{|q|}{p} \int_0^{r_{max}} B ds}$$

- Contributions to $\delta \alpha$

$$\begin{aligned} \delta \alpha &= \sqrt{(\delta \alpha_{\text{Vielfachstreuung}})^2 + (\delta \alpha_{\text{Detektorauflösung}})^2} \\ &= \sqrt{\left(\frac{13,6 \text{ MeV}}{p} \sqrt{\frac{D}{X_0}} \right)^2 + (\delta \alpha_D)^2} \end{aligned}$$

Hence

$$\frac{\delta p}{p} = \frac{13,6 \text{ MeV} \sqrt{\frac{D}{X_0}}}{|q| \int B ds} \oplus \frac{\delta \alpha_D}{|q| \int B ds} \cdot p$$

- ⇒ Best possible momentum given by the ratio of multiple scattering and the magnetic field integral.
- ⇒ High momenta (small values of α): Momentum resolution determined by the ratio of the spatial resolution of the detector and the magnetic field integral. The momentum resolution degrades with increasing p .

Requirements

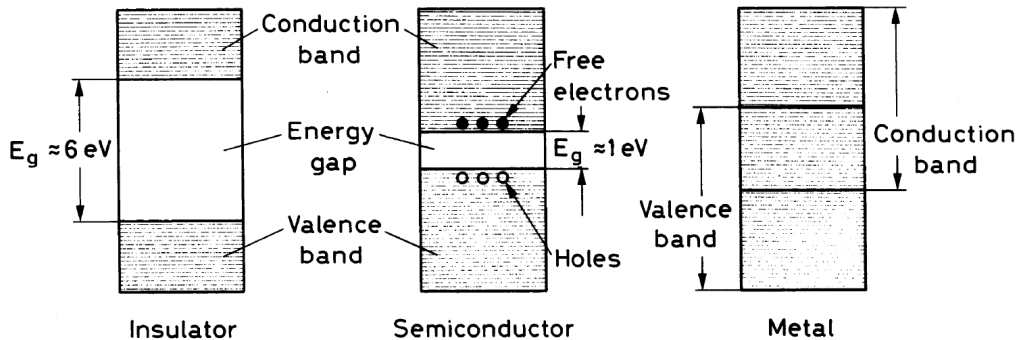
- **General requirements**
 - As little detector material as possible to minimize the multiple scattering contribution to the momentum resolution.
 - High spatial resolution to maximize the momentum resolution for highly energetic particles.
- **Additional requirements at a hadron collider**
 - High granularity to be able to separate particle trajectories even in the presence of high charged particle densities.
 - Radiation hardness.

Detector types in modern inner detectors

- **Experiments at e^+e^- colliders**
 - Highly granular semiconductor detectors close to the beam line for secondary vertex reconstruction.
 - Low- X_0 semiconductor or gaseous ionization detectors at larger distance from the beam line.
- **Experiments at hadron colliders**
 - Entire inner detector with highly granular and radiation hard semiconductor detectors.

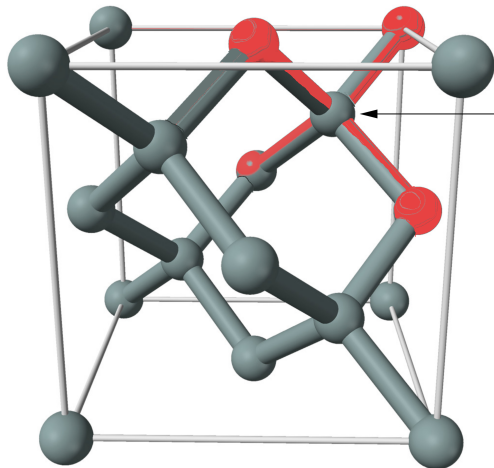
Introduction to semiconductor detectors

Energy bands in solid-state bodies



Charge carriers in semiconductors

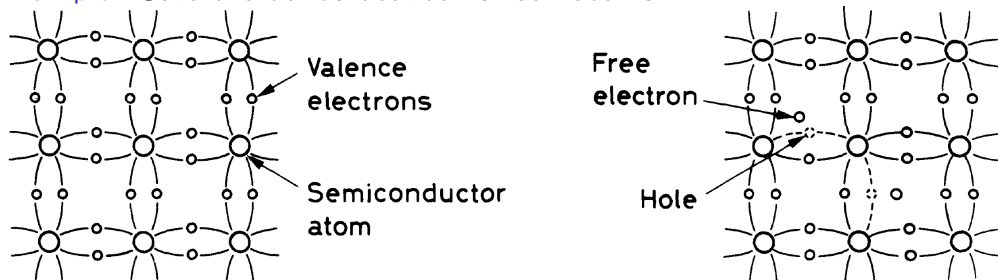
Example: Covalent bonds between silicon atoms.



Silicon atom sharing electrons with its **4 nearest neighbours**

Charge carriers in semiconductors

Example: Covalent bonds between silicon atoms.



Two source of electrical conductivity in semiconductors:

- Motion of free electrons in the conduction band

and

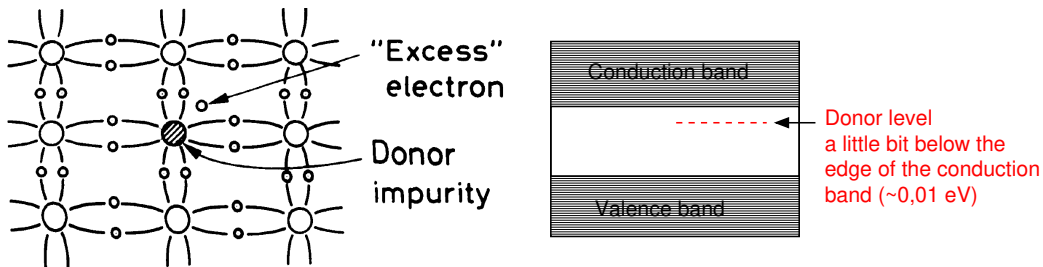
- Motion of holes in the valence band.

(Only motion of electrons in the conduction bands in conductors.)

- The number of free electrons and holes is the same in **pure semiconductors**.
- There can be more free electrons than holes and vice versa in **doped semiconductors**.

Doping of silicon with pentavalent atoms

Pentavalent atoms: arsene, phosphor, antimony.



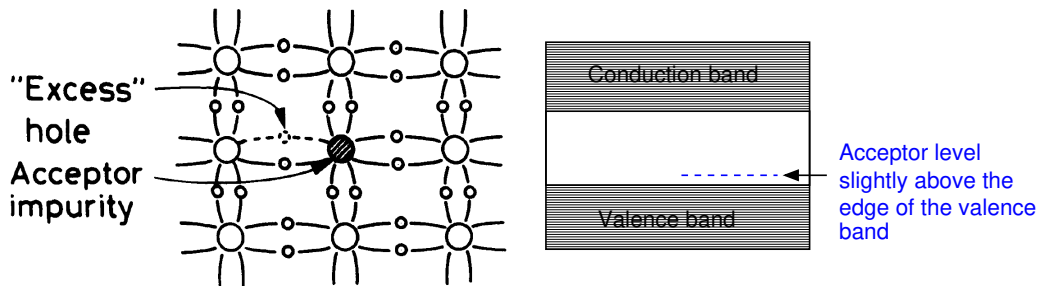
⇒ Increased conductivity due to the excess electrons which can be very easily excited thermally into the conduction band.

Nomenclature: n-type semiconductor.

Main charge carriers in an n-type semiconductor: electrons.

Doping of silicon with trivalent atoms

Trivalent atoms: gallium, boron, indium.

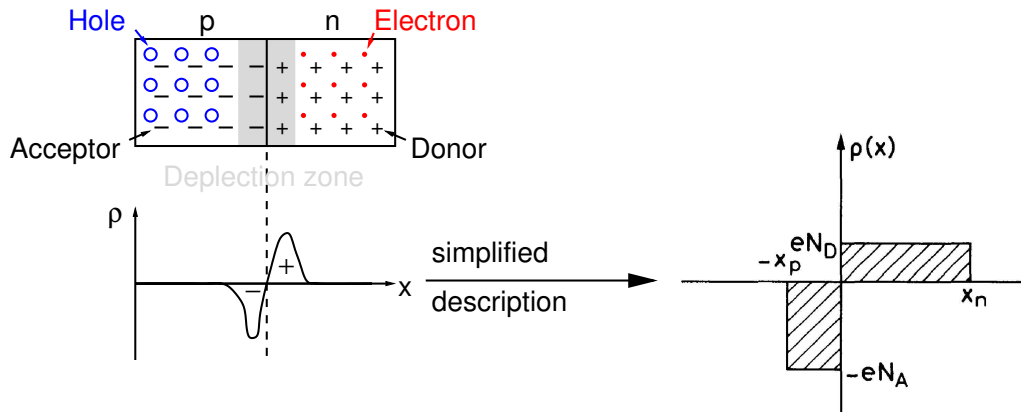


⇒ Increased conductivity due to excess holes into which valence electrons can be easily excited thermally.

Nomenklatur: p-type semiconductor.

Main charge carriers in an p-type semiconductor: holes.

The pn junction



$N_{A/D}$: Acceptor-/Donor concentration

$$\rho(x) = \begin{cases} -eN_A & (x \in [-x_p, 0]) \\ +eN_D & (x \in [0, x_n]) \\ 0, & \text{else} \end{cases}$$

$\text{div}\vec{E} = \frac{\rho}{\epsilon}$ leads to $\frac{dE}{dx} = \frac{\rho(x)}{\epsilon}$, such that

$$\begin{aligned} E(x) &= 0 \quad (x < -x_p, x > x_n), \\ E(x) &= -\frac{e}{\epsilon}N_A(x + x_p) \quad (x \in [-x_p, 0]), \\ E(x) &= +\frac{e}{\epsilon}N_D(x - x_n) \quad (x \in [0, x_n]). \end{aligned}$$

Continuity at $x = 0$ leads to

$$N_A x_p = N_D x_n \Leftrightarrow \frac{x_p}{x_n} = \frac{N_D}{N_A} \quad (*)$$

\Rightarrow The depletion zone extends further into the region of lower doping concentration.

Potential difference (so-called "contact potential")

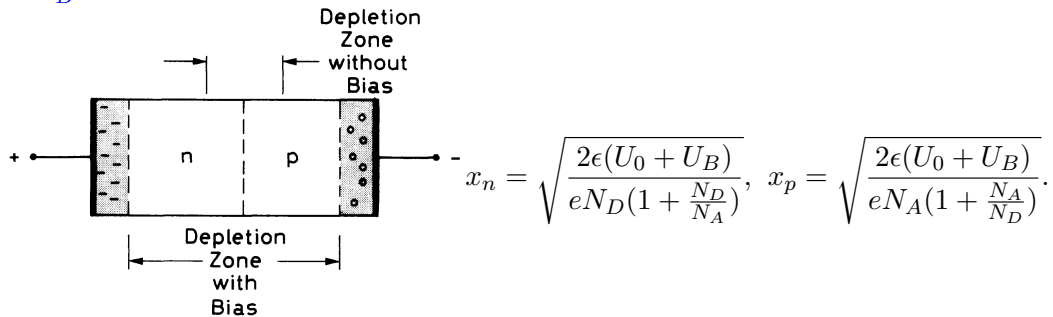
$$\begin{aligned}U_0 &= - \int_{-x_p}^{x_n} E(x) dx = + \frac{eN_A}{2\epsilon} (x + x_p)^2 \Big|_{-x_p}^0 - \frac{eN_D}{2\epsilon} (x - x_n)^2 \Big|_0^{x_n} \\ &= \frac{e}{2\epsilon} (N_D x_n^2 + N_A x_p^2)\end{aligned}$$

Size of the depletion zone

$$x_n = \sqrt{\frac{2\epsilon U_0}{eN_D(1 + \frac{N_D}{N_A})}}, \quad x_p = \sqrt{\frac{2\epsilon U_0}{eN_A(1 + \frac{N_A}{N_D})}}$$

Increasing the depletion zone

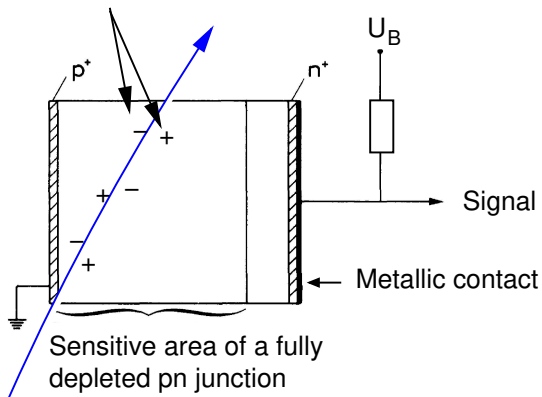
The depletion zone can be increased by applying a so-called "bias voltage" U_B :



$U_B \sim 300 \text{ V}$ for complete depletion of the pn junction.

Basic principle of a semiconductor detector

Liberated charge carriers which are pulled by the electric field towards the contact



Ionizing particle

In order to prevent the creation of an ohmic contact with a depletion zone extending far into the semiconductor, contact surfaces with highly doped layers are used.

Example: silicon strip detector for position measurements

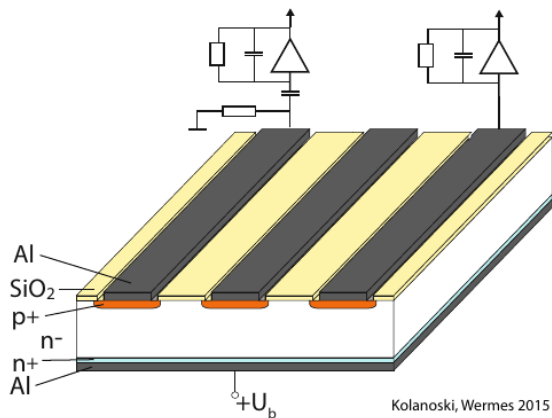


Abb. 8.36 Direkt (DC, rechts) und kapazitiv (AC, links) gekoppelte Auslese eines Streifendetektors.